I COBBIND
I CONGRESSO BRASILEIRO DE BIOTECNOLOGIA INDUSTRIAL
XXIV SINAFERM ·· XV SHEB ·· XV ENZITEC FLORIANÓPOLIS ·· 2024
Creating connections between biotechnology and industrial sustainability
August 25 to 28, 2024
Costão do Santinho Resort, Florianópolis, SC, Brazil
BIOPRODUCTS ENGINEERING

FORMULATION OF HYDROGELS FOR INJECTION AND 3D BIOPRINTING OF SCAFFOLDS FOR REGENERATIVE MEDICINE APPLICATIONS

Rodolpho F. Correa[1], Carolina C. Zuliani[2], Eronildo A. P. Junior[3], Ibsen B. Coimbra[2], Marcos A. D'Ávila[3], Ângela M. Moraes[1*]

1 School of Chemical Engineering, Department of Engineering of Materials and of Bioprocess, University of Campinas, Campinas, SP, Brazil.
2 School of Medical Science, Department of Orthopedics, Rheumatology and Traumatology, University of Campinas, Campinas, SP, Brazil.
3 School of Mechanical Engineering, Department of Manufacturing and Materials Engineering, University of Campinas, Campinas, SP, Brazil.
** ammoraes@unicamp.br*

ABSTRACT

Hydrogels consisting of the biopolymers methylcellulose (MC) and alginate (A) have potential to be used for both injection and 3D printing of scaffolds for cartilage tissue engineering to address osteoarthritis. Four formulations were developed for this purpose herein, consisting of 0, 3, 6 and 9% (w/v) of MC and 3% (w/v) of A. All formulations were characterized in terms of gelation, rheological, printability and cytotoxicity. The formulations containing 6 and 9% MC exhibited self-assembly property via sol–gel phase transition upon temperature stimuli from 25 to 37 °C. The formulation with 9% MC showed improved viscosity, shear-thinning behavior and gel-like characteristics, forming a continuous and thin filament. The metabolic activity of L929 cells in contact with extracts of all hydrogels exceeded 79%. Overall, the hydrogel comprised of 9% MC exhibited the most promising results for the aimed applications.

Keywords: Hydrogel, Injection, 3D Bioprinting, Cartilage, Osteoarthritis.

1 INTRODUCTION

Osteoarthritis (OA) is the leading form of arthritis causing adult chronic pain and disability, marked by cartilage degradation mainly affecting the hip, hands and knees.[1,2] Presently, the available therapies for OA are symptomatic and involve invasive surgeries. Aging is the main risk factor for OA, with 595 million globally registered cases in 2020, incurring an average annual cost of USD13.6k per patient.[1,2] Thus, the lack of effective treatments and the socioeconomic burden associated with OA underscore the need for novel therapeutic approaches. Tissue engineering (TE) emerges as a promising interdisciplinary area for the development of advanced biomaterials for cartilage TE. In this context, biopolymer-based hydrogels have gained attention due to their biomimetic structure, capable of incorporating cells and bioactive agents. These systems can be designed to meet the requirements for injections and 3D bioprinting of scaffolds.[3,4] Injectable hydrogels must exhibit liquid-like behavior, presenting shear-thinning and self-assembly properties through crosslinking.[3] Regarding 3D bioprinting, hydrogel bioinks must exhibit shape fidelity, where thixotropy is a relevant property.[4] For these applications, methylcellulose (MC) arises as a promising candidate due to its thermosensitive properties, enabling crosslinking at physiological temperature.[5] Regarding 3D bioprinting, MC has been blended with alginate (A), which is comprised of 1,4-linked (-D-mannuronic acid) and (-L-guluronic acid) repetitive units.[6] Alginate has been explored in bioinks due to its shear-thinning properties and crosslinking with $CaCl_2$.[7] However, to our knowledge, no studies have been reported simultaneously exploring the multifunctionality of MC and A hydrogels, what was the goal of our study.

2 MATERIAL & METHODS

To prepare the hydrogels, stock solutions of 13,5% (w/v) methylcellulose (15 cP, Sigma-Aldrich) and 9% (w/v) alginate (2,000 cP, Sigma-Aldrich) were prepared by dispersion in phosphate-buffered saline (PBS) at 550 rpm and room temperature. Then, the solutions were mixed to achieve the following concentrations: 3% MC and 3% A (formulation MC3A3); 6% MC and 3% A (MC6A3) and 9% MC and 3% A (MC9A3). As a control, a 3% (w/v) alginate hydrogel formulation (MC0A3) was also prepared. The hydrogels were sterilized by autoclaving at 121 °C and 1 atm, for 15 min, and stored overnight at 4 °C. Gelation capacity was analysed by tube inversion for 5 min at 25°C and after incubation at 37°C for 10 min. Rheological analysis was performed in a Modular Anton Paar MCR-102 rheometer equipped with a cone-plate geometry. Steady shear flow analysis was conducted with a shear rate ranging from 0.1 to 3,000 s^{-1}. Amplitude sweep analysis was carried out at a strain of 0,1 to 100% at a constant angular frequency of 10 $rad \cdot s^{-1}$. Frequency sweep analysis was conducted at an angular frequency rate ranging from 300 to 0,1 $rad \cdot s^{-1}$ at a constant strain of 1%. Step strain analysis was performed by applying a shear rate of 1 s^{-1} for 25 s following a shear rate of 100 s^{-1} for 50 s and 1 s^{-1} for 300 s. All measurements were conducted at 25°C unless otherwise stated. Hydrogel printing was conducted using the extrusion TissueStartTM 3D Bioprinter (TissueLabs) assisted by the Repetier-Host software. Printability analysis was assessed by varying the extrusion flow from 300 to 400% at a fixed printing speed of 1mm/s, using a 5mL syringe of 20G (0,91mm). Indirect cytotoxicity analysis with MTT was performed using L929 cell line following the referred procedure.[5] Results were expressed as mean ± standard deviation and differences evaluated by analysis of variance (ANOVA) with a level of significance of $p \leq 0.05$ (Tukey test).

3 RESULTS & DISCUSSION

For the tube inversion assay, at 25°C, all hydrogel formulations exhibited homogeneous liquid-like behavior (Figure 1). The increase in the concentration of MC led to a decrease in the flowing capacity, indicating a rise in the viscosity of the pre-gels.

Conversely, at 37°C, formulations comprising higher MC concentrations showed a sol-gel phase transition in response to thermal stimuli. Notably, MC9A3 exhibited a gel-like behavior with no apparent flowing capacity. Thus, the polymeric system is above the critical solution temperature (CST). In this condition, the polymer-solvent hydrogen bonds are thermally disrupted, shifting the interaction balance towards hydrophobic polymer-polymer interactions among the methyl groups of MC.[8] As a result, the polymeric system forms a semi-interpenetrated network of A entangled within the crosslinked network of MC.[9] Hence, the MC9A3 exhibits a self-assembly property by crosslinking at physiological temperature, critical for injection and 3D bioprinting.

Figure 1 Results of tube inversion depicting hydrogel gelation analysis at 25 and 37°C for: (a) MC0A3, (b) MC3A3, (c) MC6A3, (d) MC9A3.

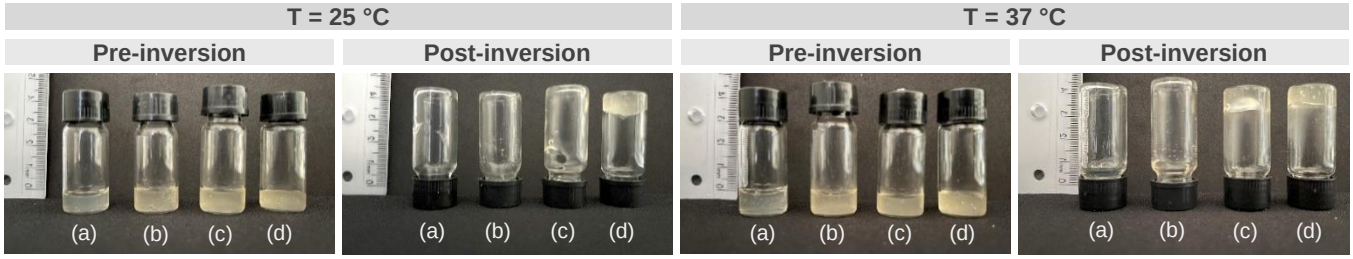

The rheological analysis was performed to characterize the flowing behavior of the hydrogels in their pre-gel state at 25°C (Figure 2). For the steady shear flow analysis, all hydrogel formulations exhibited non-Newtonian behavior, demonstrating shear-thinning characteristics, desired for injection and 3D printing (Figure 2a). Conversely, the A control hydrogel displayed a plateau in viscosity at lower shear rates, indicating Newtonian behavior, which transitioned to shear-thinning at higher shear rates. Also, the increase in MC concentration correlated with an increase in both viscosity and shear-thinning behavior, where MC9A3 showed the highest values. This could be justified by a rise in hydrogen bonding among the hydroxyl groups of MC and A. For the amplitude sweep analysis, all hydrogels exhibited a linear viscosity region (LRV) along the strain interval (Figure 2b). Thus, both storage (G') and loss (G'') modulus remained independent of strain with G''>G', suggesting a liquid-like behavior. In the frequency sweep, G''>G' for all formulations except MC9A3, with non-intersecting values, showing gradual increases with angular frequency (Figure c). The same effect of increasing concentration of MC was observed in the strain and frequency sweeps. In both cases, increasing MC correlated with a reduction in G' and G'' differences, notably increasing the characteristic of gel at MC9A3. For the step strain analysis, all hydrogels exhibited a rapid decrease in viscosity in response to strain, corroborating with their shear-thinning behavior (Figure 2d). Following 30 s of relaxation, hydrogels showed viscosity recovery of 65%, 72%, 86% and 100% for MC9A3, MC6A3, MC3A3 and MC0A3, respectively.[10] In this condition, the polymeric systems recover their entangled conformation by re-establishing the hydrogen bonds among MC and A, disrupted during extrusion. Furthermore, increased polymeric concentrations resulted in a prolonged structural and viscosity recovery, correlating with higher levels of possible hydrogen bonding configurations. Our findings suggest that the hydrogels exhibited a slow thixotropic recovery behavior, which could potentially result in low shape fidelity in 3D printing.

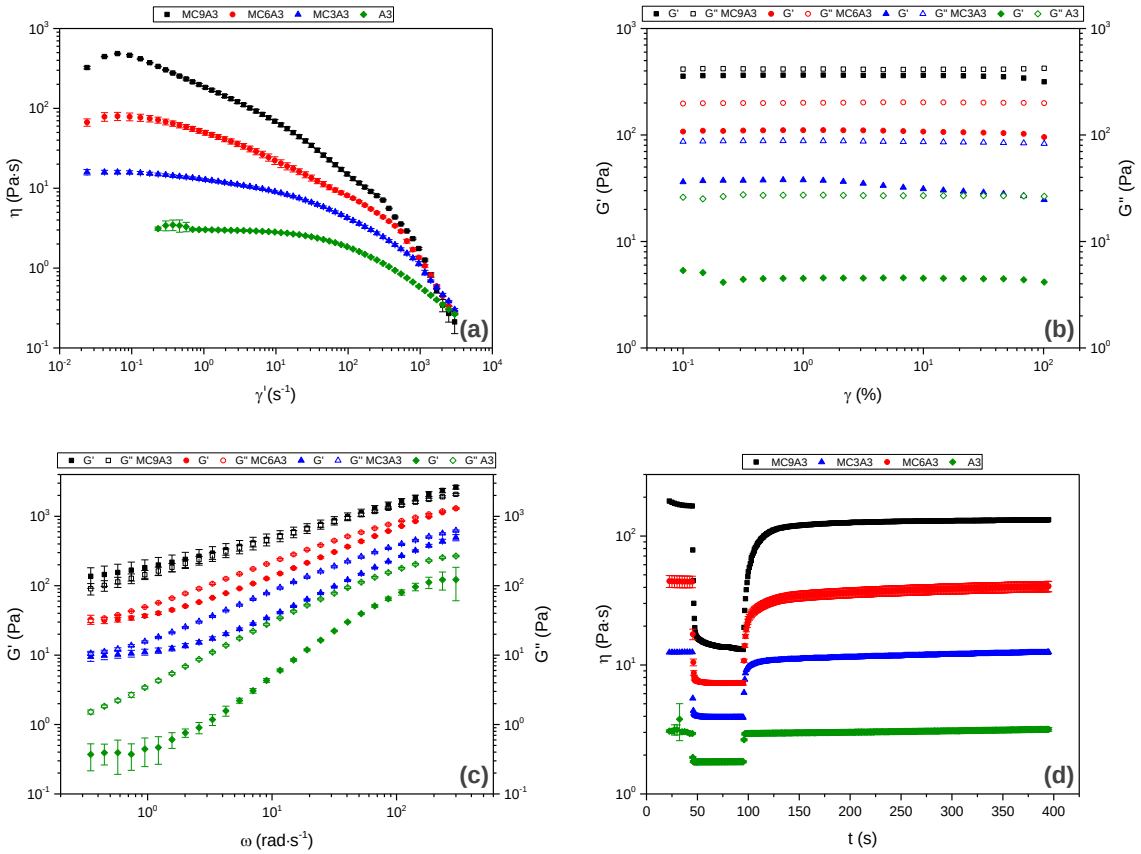

Figure 2 Rheological analysis for hydrogel formulations: (a) Steady shear flow measurements correlating viscosity (η) with shear rate (γ'); (b) Amplitude sweep measurements correlating storage (G') and loss (G'') modulus with strain (γ); (c) Frequency sweep measurements correlating G' and G'' with angular frequency rate (ω); (d) Step strain measurements correlating η with time (t).

Printability analysis was performed to investigate filament formation of hydrogels using an extrusion 3D printer (Table 1). Our results show that only the polymeric blends enabled filament formation. Hydrogels with higher MC concentrations resulted in continuous and thinner filaments at 400% extrusion flow, consistent with the rheological analysis. Particularly, MC9A3 presented the thinnest and most continuous filament with no apparent coalescence, suitable for 3D printing of scaffolds.

Table 1 Representation of the printability analysis depicting filament formation at 300 and 400% extrusion flow at a printing speed of 1mm/s.

Extrusion Flow (%)	MC0A3	MC3A3	MC6A3	MC9A3
300	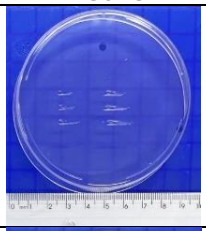	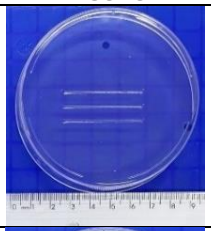	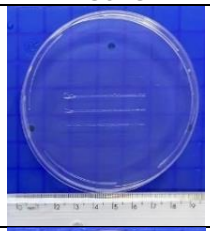	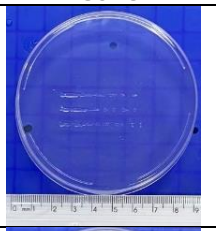
400	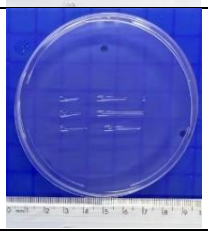	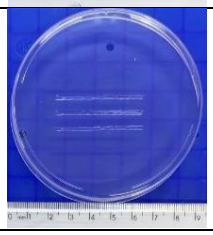	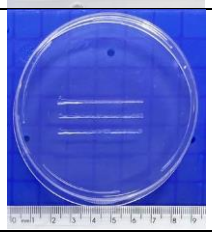	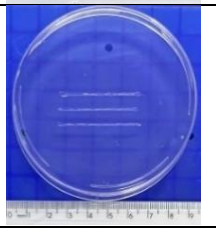

Indirect cytotoxicity analysis was performed to determine the proliferation of L929 cells after contact with hydrogel extracts for 24 h (Figure 3). Mitochondrial metabolic activity levels above 79% were observed for cells exposed to all hydrogel extracts, with no statistical differences being observed. These results suggest that, according to ISO 10993-5 (2009), none of the formulations are cytotoxic.

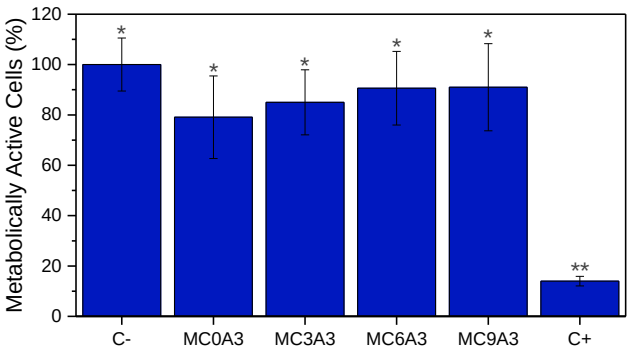

Figure 3 Indirect MTT cytotoxicity analysis of L929 cells after contact with hydrogel extracts for 24 h. Different symbols indicate a statistical difference with a level of significance of $p \leq 0.05$ (Tukey test).

4 CONCLUSION

The hydrogel formulation composed of 9% MC and 3% A exhibited the most promising results in terms of self-assembly, shear thinning and thixotropic properties suitable for injection and 3D bioprinting. Notably, MC9A3 underwent sol-gel phase transition via thermal crosslinking at physiological temperatures, displayed shear-thinning liquid-like behavior, and exhibited thixotropic properties with a 65% viscosity recovery. Printability analysis showed that increasing the MC concentration resulted in thin, continuous filaments. The formulation MC9A3 yielded the most promising filaments, without apparent coalescence. Furthermore, all hydrogel formulation extracts were non-cytotoxic. Therefore, the MC9A3 formulation, fully based on polysaccharide molecules, seems to be a very satisfactory multifunctional hydrogel, suitable for incorporating bioactive compounds and cells, for injection and 3D bioprinting of scaffolds, with high potential to contribute to the advance in cartilage TE technology.

REFERENCES

1 STEINMETZ, J. D. GLOBAL BURDENS OF DISEASE, C. 2023. Lancet Rheumatol. 5. 508–522.
2 LEIFER, V. P., KATZ, J. N. LOSINA, E. 2022. Osteoarthr. Cartil. 30(1). 10-16.
3 GUVENDIREN, M. LU, H. D. BURDICK, J. A. 2012. Soft Matter. 8(2). 260-272.
4 HERNÁNDEZ-GONZÁLEZ, A. C. TÉLLEZ-JURADO, L. RODRÍGUEZ-LORENZO, L. M. 2020. Carbohydr. Polym. 229.
5 WESTIN, C. B. NAGAHARA, M. H. T. DECARLI, M. C. KELLY, D. J. MORAES, A. M. 2020. Eur. Polym. J. 129.
6 KILIAN, D. AHLFELD, T. AKKINENI, A. R. BERNHARDT, A. GELINSKY, M. LODE, A. 2020. Sci. Rep. 10(1). 1–17.
7 DECARLI, M. C. SEIJAS-GAMARDO, A. MORGAN, F. L. C. WIERINGA, P. BAKER, M. B. DA SILVA, J. V. L. MORAES, A. M. MORONI, L. MOTA, C. 2023. Adv. Healthc. Mater. 12(19).
8 BONETTI, L. NARDO, L. D. FARÈ, S. 2021. Tissue Eng. Part B Rev. 27(5). 486–513.
9 ESTEVAM, B. R. PEREZ, I. D. MORAES, A. M. FREGOLENTE, L. V. 2023. Mater. Today Chem. 34.
10 HERRADA-MANCHÓN, H. FERNÁNDEZ, M. A. AGUILAR, E. 2023. Gels. 9(7). 517.

ACKNOWLEDGEMENTS

The authors acknowledge the support from the National Council for Scientific & Technological Development (CNPq, Brazil – Grants # 141734/2023-0 and 314724/2021-4) and the São Paulo Research Foundation (FAPESP, Brazil – Grant # 2022/12970-3).